SCIENCE CHINA
Physics, Mechanics & Astronomy

• Research Paper •
Special Topic: Magnetic Materials at Nano-scale

July 2011 Vol.54 No.7: 1200–1207
doi: 10.1007/s11433-011-4356-3

Microwave magnetic properties of soft magnetic thin films

CHAI GuoZhi, GUO DangWei, FAN XiaoLong & XUE DeSheng*

Key Lab for Magnetism and Magnetic Materials of the Ministry of Education, Lanzhou University, Lanzhou 730000, China

Received December 15, 2010; accepted February 15, 2011; published online May 24, 2011

We review our works that focus on the microwave magnetic properties of metallic, ferrite and granular thin films. Soft magnetic material with large permeability and low energy loss in the GHz range is a challenge for the inforcom technologies. GHz magnetic properties of the soft magnetic thin films with in-plane anisotropy were investigated. It is found that several hundreds of permeability at the GHz frequency was achieved for $Co_{100-x}Zr_x$ and $Co_{90}Nb_{10}$ metallic thin films because of their high saturation magnetization, and an adjustable resonance frequency from 1.3 to 4.9 GHz was obtained. Compared with the metallic thin films, the weaker saturation magnetization of Ni-Zn ferrite thin films results in several tens of permeability at the GHz frequency, but the larger resistivity of the ferrite prepared *in situ* without any heating treatments has lower energy loss. In order to obtain materials with large permeability and low energy loss in the GHz range, the [CoFe-NiZn ferrite] composite granular thin films were investigated, where the advantage of higher saturation magnetization for the metallic alloy and the high resistivity as well as high saturation magnetization for the ferrite results in a good GHz magnetic performance.

microwave magnetic properties, metallic thin films, ferrite thin films, granular thin films, in-plane uniaxial anisotropy

PACS: 75.30.Gw, 75.70.Ak, 75.40.Gb, 76.50.+g, 78.70.Gq

Soft magnetic thin films with excellent high frequency characteristics are strongly required as core materials used in magnetic components for the ceaseless increase of the working frequency of the data transmission and multiple accesses in computer, mobile and blue-tooth devices [1–6]. The basic demands for these magnetic materials are GHz resonance frequency, high permeability and low energy loss at GHz. The investigation of GHz dynamic properties of the magnetic materials is currently attracting significant attention. It has been known since the work of Acher that GHz resonance frequency f_r and high permeability can be achieved for thin films with in-plane uniaxial anisotropy [7,8]. For these thin films, high saturation magnetization $4\pi M_s$ and adjustable uniaxial anisotropic field H_k are key to optimizing f_r and permeability which can be written as [9]:

$$\mu = \frac{4\pi M_s}{H_k} + 1, \quad f_r = \frac{\gamma}{2\pi}\sqrt{4\pi M_s H_k}, \tag{1}$$

where γ is the gyromagnetic factor. However, the investigation of the thin films with adjustable GHz resonance frequency and high permeability at GHz is still a challenge, especially for the thin film with high resistivity at the same time.

Magnetic metals (Fe, Co, Ni, and their alloys) are those materials with high saturation magnetization $4\pi M_s$. We prepared $Co_{100-x}Zr_x$ and $Co_{90}Nb_{10}$ thin films to obtain high permeability and resonance frequency [10,11]. For the $Co_{100-x}Zr_x$ and $Co_{90}Nb_{10}$ alloys, $4\pi M_s$ is fixed. As shown in eq. (1), both μ and f_r are determined by H_k. We studied the adjustable behavior of H_k for thin films deposited at different oblique angles. Consequently, an optimization of μ and f_r for the $Co_{90}Nb_{10}$ films was achieved. However, it is difficult to reduce the eddy current loss of magnetic metals.

As an insulator, ferrites are widely used due to their weak

*Corresponding author (email: xueds@lzu.edu.cn)

eddy current loss at GHz. Ni-Zn ferrite thin films which have the highest $4\pi M_s$ in ferrites were investigated. To our knowledge, the soft ferrite films deposited by many methods [12–17] require high temperature post-heating treatments or substrate heating at least of 600°C to obtain a better spinel structure and soft magnetic properties, which is impossible for electronic circuit integrations. We report the achievement the *in-situ* fabrication of Ni-Zn ferrite films with well-defined spinel crystal structure at room temperature without any heating treatments by magnetron sputtering [18,19]. Compared with the magnetic alloy, the lower $4\pi M_s$ and more difficult control of the anisotropic field result in lower μ and f_r.

The metallic thin films were investigated to obtain high M_s but with lower resistivity; the ferrite thin film was investigated to obtain high resistivity but with lower M_s. For thin films with both high resistivity and high GHz magnetic properties, most of the *K*–*M*–*X* structure films have been reported [20–25], where *K* stands for magnetic metals (Fe, Co, Ni, and their alloys), *M* for nonmagnetic elements (Hf, Mg, Al, Si, Zr, etc.) and *X* for second period elements (N, O, F) [26,27]. As the insulated phase formed in the thin film is a nonmagnetic material, it is difficult to realize a granular film with both M_s and high resistivity. Here, we used the NiZn ferrites with electric insulating and magnetic properties as the adulterant for granular films [28]. The high permeability in GHz frequency and low energy loss can be achieved by optimizing the component and the micro structure of the thin films.

The rest of this paper is organized as follows. In the next section, the experimental details and the measurement techniques employed in the characterization of thin films are given. In sect. 3 we give the GHz magnetic properties of metallic, ferrite and granular thin films and discuss the relationships between structure and permeability in GHz. We finish with a brief conclusion where we place in a broader perspective the relevance of the content of this paper.

1 Experimental details

All the soft magnetic thin films were prepared by radio frequency (rf) sputtering onto 10 mm×20 mm×0.42 mm (111)-oriented Si substrates attached to a water-cooling system at room temperature with background pressure lower than 5×10^{-5} Pa. A Co target, 70 mm in diameter and 3 mm in thickness, on which Zr or Nb chips were placed in a regular manner, is kept and the substrate distance as 9.0 cm was used to deposit $Co_{100-x}Zr_x$ and $Co_{90}Nb_{10}$ thin films. For $Co_{100-x}Zr_x$, $Co_{90}Nb_{10}$ thin films, the samples were deposited at an angle with substrate normal to attain uniaxial anisotropy [29]. During sputtering, an Ar flow rate of 20 SCCM (SCCM denotes cubic centimetre per minute at STP) was needed to maintain an Ar pressure of 0.15 Pa, and the rf power density was 1.7 W/cm^2. A $Ni_{0.5}Zn_{0.5}Fe_2O_4$ ferrite target, with 76 mm in diameter and 3 mm in thickness, on which $NiFe_2O_4$ and $ZnFe_2O_4$ ferrite chips were placed in a regular manner, was used to deposit Ni-Zn ferrite thin films. A Co target, 70 mm in diameter and 3 mm in thickness, on which Fe chips and $Ni_{0.5}Zn_{0.5}Fe_2O_4$ chips were placed in a regular manner, was used to deposit $(Co_{0.65}Fe_{0.35})_{1-x}(Ni_{0.5}Zn_{0.5}Fe_2O_4)_x$ composite granular films. The composition of the deposited films was adjusted by controlling the number of the chips on the targets. The samples were placed at a perpendicular position with the target. The RF power density was 4.4 W/cm^2 and a mixed gas of argon (Ar) and oxygen (O_2) was used during sputtering. The sputtering pressure was kept at 2.0 Pa. The $(Co_{0.65}Fe_{0.35})_{1-x}(Ni_{0.5}Zn_{0.5}Fe_2O_4)_x$ thin films were deposited with the same condition as $Co_{100-x}Zr_x$, $Co_{90}Nb_{10}$ thin films.

The compositions of the films were measured by energy dispersive X-ray spectroscopy (EDS). The crystallographic and microstructure properties of the films were characterized by X–ray diffraction (XRD, X′ Pert PRO PHILIPS with CuK$_\alpha$ radiation) and a field emission scanning electron microscope (SEM, Hitachi S-4800), respectively. The magnetic hysteresis loops of the films were measured at room temperature using a vibrating sample magnetometer (VSM, Lakeshore 7304 model). The direction of the applied magnetic field was parallel to the film plane. $\mu_0 M_s$ and H_c were obtained from the loops. Permeability spectra were carried out with a PNA E8363B vector network analyzer using the microstrip method from 100 MHz to 8 GHz with the sample positioned in the middle of the strip line [30]. All the above observations and measurements were performed on as-deposited samples at room temperature.

2 Results and discussion

2.1 $Co_{100-x}Zr_x$ and $Co_{90}Nb_{10}$ thin films

Figure 1 shows the hysteresis loop, the magnetic spectrum and the morphology of the Co and $Co_{92}Zr_8$ thin films deposited obliquely on Si (111) at 23°. The saturation magnetization of Co film is about 1.6 T, which is slightly less than bulk value ~1.7 T in Co. The coercive force H_c is 19.3 mT along the easy axis (EA) and 16.9 mT along the hard axis (HA) can be obtained from Figure 1(a). The hysteresis loops indicate that these Co thin films do not have well in-plane uniaxial anisotropy. As a consequence, the permeability in GHz is low for these Co thin films as shown in Figure 1(b). The particle size of these films is about 30 nm as shown in Figure 1(c). However, after doping a small amount of Zr, the $Co_{92}Zr_8$ films display excellent soft magnetic properties and well-defined in-plane uniaxial anisotropy, as shown in Figure 1(d). The loop along EA is basically a rectangle, which indicates that in the remanence state the magnetization aligns almost along the EA direction. The H_c along EA (H_{ce}) is less than 0.15 mT, meaning that the re-orientation of magnetization easily occurs by applying a relatively small field along that direction. The HA loop is basically a close curve without hysteresis, indicating that the change in magnetization takes place through its rotation by field. For this film, in-plane uniaxial anisotropic field H_k is about 11.5 mT, and the saturation magnetization is about 1.3 T. The results shown in Figure 1 demonstrate that the introduction of Zr into obliquely deposited Co films can significantly decrease H_{ce} and simplify the domain structure and magnetization process. The spectra in Figure 1(e) show frequency dependences of the real (μ') and imaginary (μ'') components of the relative permeability of the $Co_{90}Zr_8$ films. The resonance-type permeability spectra show that the natural resonance frequency f_r is 3.4 GHz. The average grain size of films decreases from 30 nm to less than 10 nm with doping 8% Zr element as shown in Figure 1(f).

It is speculated that such a profound improvement of soft magnetic properties results from the small effective magneto-crystalline anisotropy in an assembly of column grains, which arises from the effect of exchange coupling between the grains. According to the random anisotropy model [25], the effective anisotropy constant K_{eff} decreases with decreasing the crystal size D. Therefore, given that the magnetocrystalline anisotropy has been substantially weakened, the shape anisotropy of thin film and the obliquely-induced anisotropy which places magnetization along the in-plane EA become dominant. As a result, the soft magnetic properties and high permeability in GHz have been optimized.

In order to adjust the in-plane uniaxial anisotropic field, we have studied the oblique angle dependence of the static properties of $Co_{100-x}Zr_x$ thin films, as shown in Figure 2. Figure 2(a) shows the hysteresis loops of the hard axis with different oblique angles of $Co_{93}Zr_7$. As expected, a monotone increase of H_k as a function of oblique angle can be observed. For instance, H_k for $Co_{93}Zr_7$ film deposited at 37° is about 15.8 mT, almost ten times larger than 1.6 mT found for the film deposited at normal incidence. H_{ce} of the films keeps low values ~0.1 mT which is insensitive to the deposition angle. The similar dependence can also be found for different Zr contents. We also investigate the oblique angle dependence of $Co_{90}Nb_{10}$ thin films, and the result shows an increasing H_k with an oblique angle similarly. Therefore, we can adjust the in-plane uniaxial anisotropic field by controlling the oblique angle in those films. And H_{ce} of the films keeps low values ~0.1 mT for all the $Co_{100-x}Zr_x$ and $Co_{90}Nb_{10}$ thin films which are insensitive to the deposition angle.

Frequency dependences of the real (μ') and imaginary (μ'') components of the relative permeability of the $Co_{93}Zr_7$ films are shown in Figure 3. High permeability in GHz has been obtained for these films as shown in Figure 3(a). As eq. (1) indicates, the increase of H_k results in f_r value in a much higher frequency and keeps μ still at a high level. For example, for the film deposited at ~0° with small H_k, μ' keeps a high value ~500 up to 1 GHz, as shown in Figures 3(a) and 3(b), and f_r is around 1.7 GHz, which causes a significant magnetic loss and a sharp decrease of μ' and increase of μ''. However, for the film deposited at ~37° with large H_k, f_r can attain a value as high as 4.3 GHz, but μ' remains a moderate value from ~150 up to 3.5 GHz, as shown in Figures 3(a) and 3(b).

Therefore, by flexibly adjusting the oblique angle, the resonance frequency can be manipulated in a wide frequency range, as shown in Figure 3(c). Thus, an optimal balance between permeability and resonance frequency can be achieved, which is important for soft magnetic films in high frequency applications. Similarly, the increase of H_k results in a significant enhancement in the resonance frequency of CoNb films and other compositions of CoZr thin films, as shown in Figures 3(c) and 3(d).

2.2 Ni-Zn ferrite thin films

Metals are known as conductors. The resistivity is so low that the eddy current loss is very large. Ni-Zn ferrite thin films as insulators were investigated to increase the resistivity. For ferrite prepared in room temperature, well spinel crystal structure is the precondition to obtain well magnetic properties. We study the preparing condition of $Ni_{0.4}Zn_{0.6}Fe_2O_4$ thin films as-deposited at room temperature. Figure 4 shows the X-ray diffraction (XRD) patterns of $Ni_{0.4}Zn_{0.6}Fe_2O_4$ thin films as-deposited at room temperature in the different partial pressure ratios of the argon to oxygen gas ($P_{Ar}:PO_2$). It shows that all the samples are well-crystallized and single-phase with spinel crystal structure. Observation of only selected peaks is seen in all the samples which usually appear in ferrite films [15,31]. It is worth noting that with the increase of $P_{Ar}:PO_2$ the (311) peak shifts to a larger diffraction angle and its width becomes narrow. This reveals that the larger the ratio, the better, the crystallization of spinel particles. It could be ascribed to the microstructure of films in different sputtering conditions. In order to investigate the microstructure of the ferrite films, we carried out a SEM study on all the films as a function of the $P_{Ar}:PO_2$ as shown in Figure 5. It is found that all the samples consist of particles nanocrystalline in nature and the sizes increase as the ratio increases in a range of 10–25 nm, which is consistent with Figure 4. With the $P_{Ar}:PO_2$ as 4:1, we prepared the $Ni_xZn_{1-x}Fe_2O_4$ ($0.28 \leqslant x \leqslant 0.70$) thin films with different x to study the effect of the component. For the $Ni_xZn_{1-x}Fe_2O_4$ thin films, the XRD peaks shift to large diffraction angles with the Ni concentration increasing as shown in Figure 6.

We also investigate the high frequency properties of these thin films. Figure 7 shows the frequency dependence of the complex permeability spectra for $Ni_xZn_{1-x}Fe_2O_4$ ($0.28\leqslant x\leqslant 0.70$) thin films in the range of 170 MHz –5.5 GHz. The real part of permeability μ' decreases from 20.5 to 7 with the Ni content x increasing, while the resonance frequency f_r

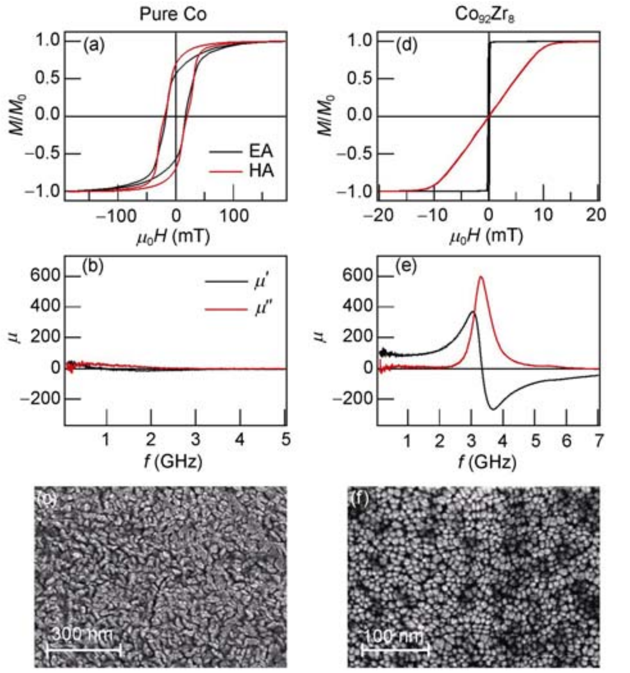

Figure 1 In-plane hysteresis loops ((a) and (d)), red line for the hard axis and black line for the easy axis; permeability spectra ((b) and (e)), black line for the real part and red line for the imaginary part; and surface images ((c) and (f)) for Co film (left column) and $Co_{92}Zr_8$ film (right column). Both of the samples were deposited at 23° [10].

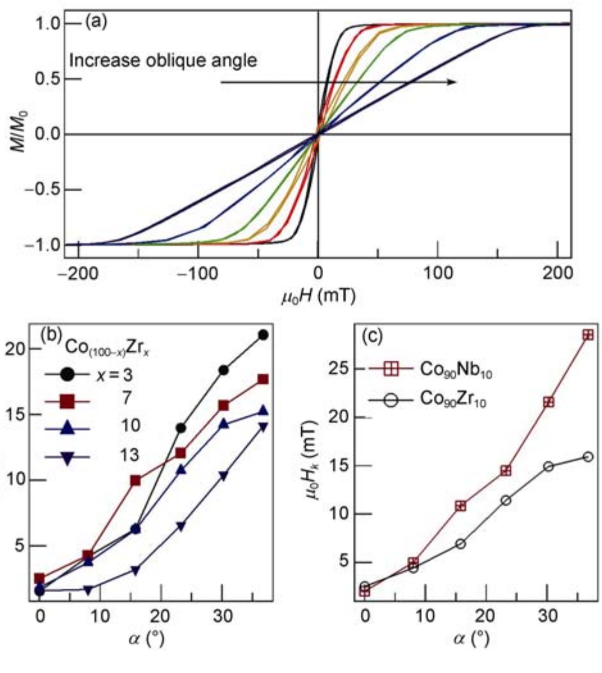

Figure 2 (a) Hysteresis loops of the hard axis for $Co_{93}Zr_7$ soft magnetic films with different oblique angles. (b) and (c) In-plane uniaxial anisotropic field of $Co_{100-x}Zr_x$ and $Co_{90}Nb_{10}$ soft magnetic films as a function of oblique angle.

around which the imaginary part of permeability μ'' reaches a maximum increases from 1.85 GHz up to 4.3 GHz. Especially, the ferrite film with optimized $x = 0.45$ has a large μ' of 15 and f_r of 2.8 GHz because of its having the largest $\mu_0 M_s$ of 0.459 T. The downshift in the μ' with the increase of Ni content x could be attributed to the increase of Ni, which increases the effective magnetic anisotropy of the ferrite films [18]. μ'' of all the films have large values in the gigahertz range; especially the ferrite film with $x = 0.28$ has a value of above 20 in a wide frequency range between 1.25 and 3.65 GHz and the maximum value of 33.5 at $f_r = 1.85$ GHz. It is seen that the resonance frequency f_r of all the films is much higher than the ferrite bulks and exceeding Snoek's limit for the Ni-Zn ferrite bulk [18].

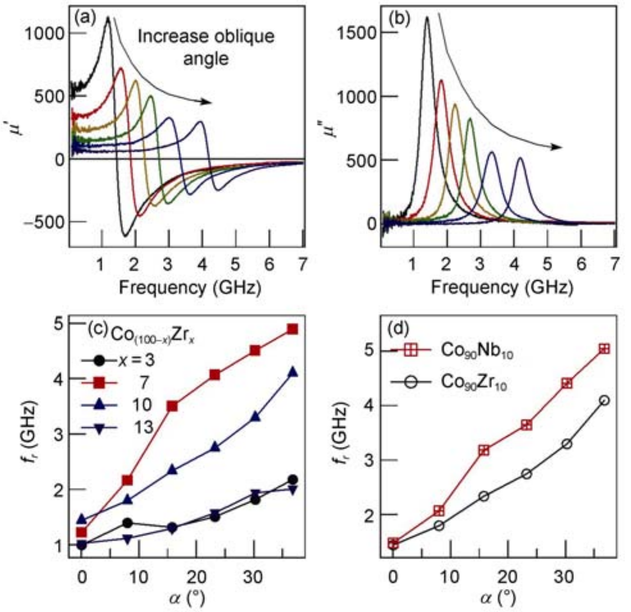

Figure 3 Frequency dependence of the relative complex permeability of $Co_{93}Zr_7$ films deposited at oblique angles from 0° to 37° ((a) for the real part and (b) for the imaginary part, respectively). The resonance frequency of $Co_{100-x}Zr_x$ (c) and $Co_{90}Nb_{10}$ (d) soft magnetic films as a function of oblique angle is also shown.

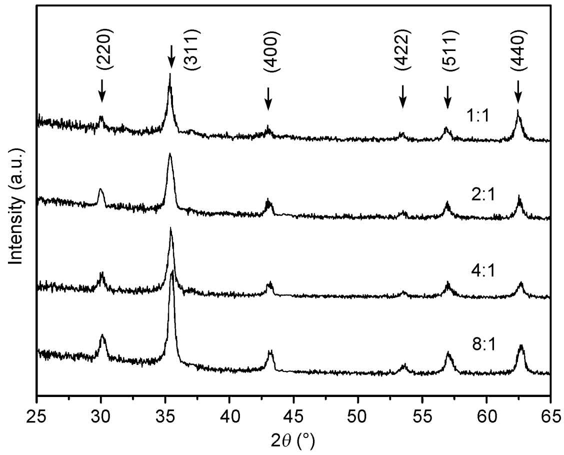

Figure 4 XRD patterns of ferrite films deposited in the different partial pressure ratios of argon to oxygen gas [18].

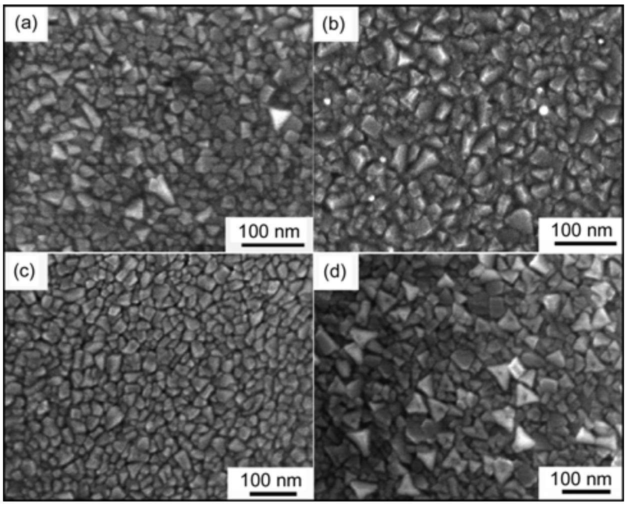

Figure 5 SEM images for ferrite films deposited in the partial pressure ratios of argon to oxygen gas of (A) 1:1, (B) 2:1, (C) 4:1 and (D) 8:1 [18].

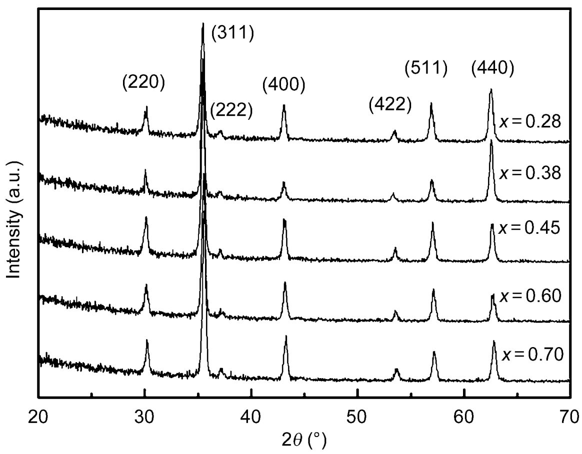

Figure 6 XRD patterns of $Ni_xZn_{1-x}Fe_2O_4$ thin films with different Ni content *x*. Indices show diffraction peaks for the spinel structure [19].

2.3 $(Co_{0.65}Fe_{0.35})_{1-x}(Ni_{0.5}Zn_{0.5}Fe_2O_4)_x$ composite granular films

The low permeability resulting from the low M_s limits the GHz application of Ni-Zn ferrite thin films. So, thin films with both high M_s and high resistivity need to be obtained. The metals have high M_s and adjustable H_k but with small resistivity, and ferrites have high resistivity but with small M_s and hardly adjustable H_k, even though Ni-Zn ferrite is the highest M_s material of ferrite. In order to obtain thin films with high resonance frequency, permeability and resistivity, we prepared the $(Co_{0.65}Fe_{0.35})_{1-x}(Ni_{0.5}Zn_{0.5}Fe_2O_4)_x$ composite granular films. Figure 8 shows the XRD patterns of these films with a different fraction of $Ni_{0.5}Zn_{0.5}Fe_2O_4$ *x*. From Figure 8, it can be seen that the bcc structure $Co_{0.65}Fe_{0.35}$ is the main phase in the films. Pure $Co_{0.65}Fe_{0.35}$ films show a bcc crystalline lattice structure with the (110), (200) and (211) peaks. For all samples, the bcc structure can

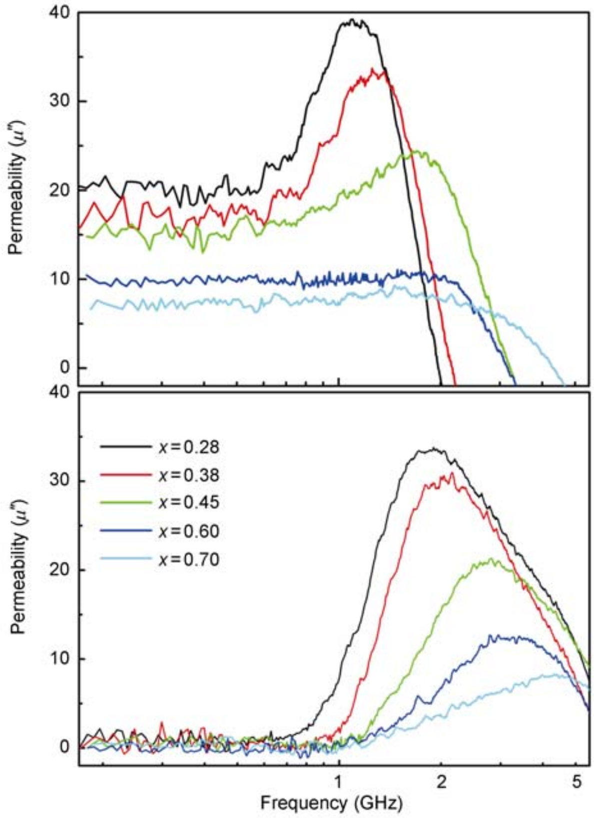

Figure 7 Complex permeability spectrums for $Ni_xZn_{1-x}Fe_2O_4$ thin films with different Ni content *x* [19].

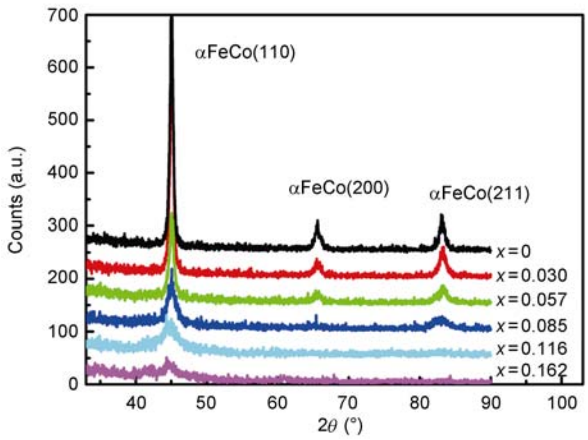

Figure 8 GIXRD spectra of $(Co_{0.65}Fe_{0.35})_{1-x}(Ni_{0.5}Zn_{0.5}Fe_2O_4)_x$ composite granular films with different fraction *x* [28].

be found, but no peaks seem related with oxides. This indicates that the fractions of ferrite are too small to be show in XRD spectra, or the crystalline structure of ferrite is not very well. It is known that the grain sizes are in inverse proportion to the peak width of X-ray diffraction by the Scherrer Equation [32]. It can be seen that for $(Co_{0.65}Fe_{0.35})_{1-x}(Ni_{0.5}Zn_{0.5}Fe_2O_4)_x$ composite granular films, the smaller $Co_{0.65}Fe_{0.35}$ grain, the larger, the value of *x* gets.

These behaviors can also be seen in SEM patterns in Figure 9.

Figure 10 shows the coercivities of easy axis and hard axis H_{ce}, H_{ch} and in-plane anisotropy H_k as a function of fraction x. For samples with x = 0 and x = 0.030, the magnetic hysteresis loops show no in-plane uniaxial anisotropy and the large coercivities are 2.68 mT and 3.24 mT, the coercivity of the latter larger than that of the former. For x = 0.057, the samples show weak in-plane uniaxial anisotropy with H_k = 4.08 mT, H_{ce} = 3.04 mT and H_{ch} = 1.02 mT, respectively. For this sample, the weak anisotropy is caused by the shape of grains and the exchange coupling between neighboring grains. For the fraction with 0.085 and 0.116, the strong exchange coupling between granules and small

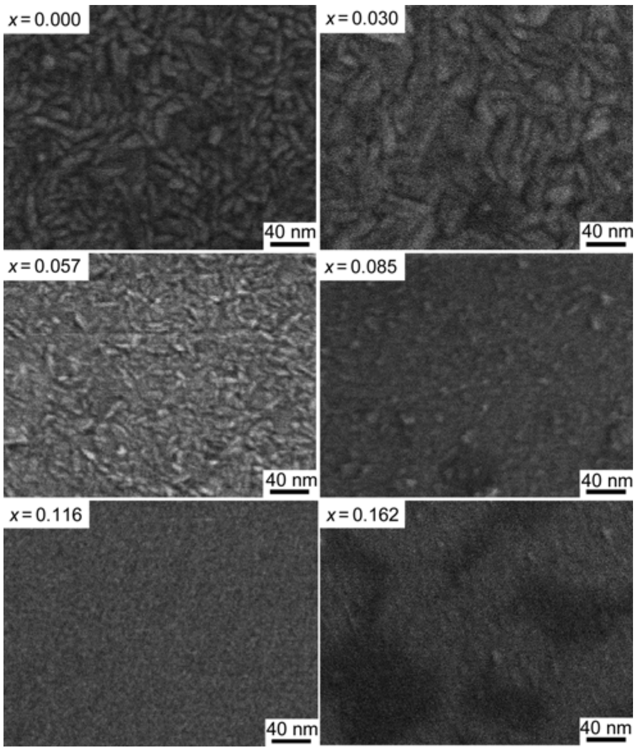

Figure 9 SEM images for $(Co_{0.65}Fe_{0.35})_{1-x}(Ni_{0.5}Zn_{0.5}Fe_2O_4)_x$ composite granular films with different fraction x [28].

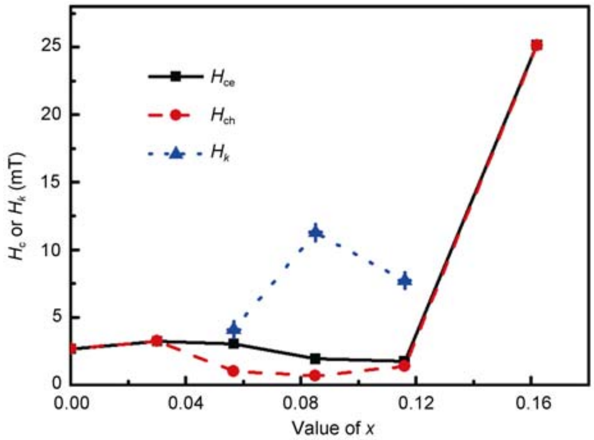

Figure 10 The coercivity of easy axis and hard axis H_{ce}, H_{ch} and in-plane anisotropy field H_k as a function of the components of $Ni_{0.5}Zn_{0.5}Fe_2O_4$ [28].

magnetocrystalline anisotropy induce the good soft magnetic properties. For samples with x = 0.085 and 0.116, H_k = 11.3 mT and 7.72 mT, H_{ce} = 1.92 mT and 1.73 mT, and H_{ch} = 0.68 mT and 1.39 mT, respectively. For sample with x = 0.162, the thin films show very large coercivity as 25.1 mT. This coercivity has the same quantity with the magnetocrystalline anisotropy field. It means that there are no exchange couple interactions between granules.

The magnetic spectra of the samples with in-plane uniaxial anisotropy are shown in Figure 11. The spectra were fitted by using theoretical spectra which were determined by the Landau-Lifshitz-Giblbert equation [33]. When x increases, significant changes can be found for the magnetic spectrums. This behavior can be described with the Kittel equation (eq. 2) for magnetic resonance. With this equation, it is easy to know that the resonance frequency increases while M_s and H_k increases. For these three samples, the values of M_s are 1.59 T, 1.41 T and 1.19 T, and the values of H_k are 4.08 mT, 11.3 mT and 7.72 mT. Because the changes of H_k are much larger than M_s and the changes of magnetic spectrum were mainly caused by H_k, the magnetic spectrum of sample with x = 0.085 shows the largest resonance frequency and lowest permeability.

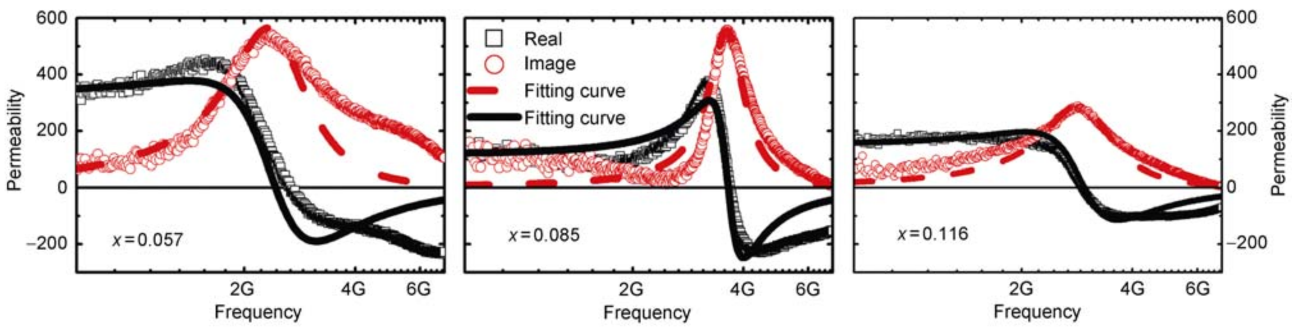

Figure 11 Dependence of complex permeability on the frequency for the samples with x = 0.057, 0.085 and 0.116. The black solid lines and red dashed lines show the fitting curve of real parts and imaginary parts of permeability as a function of frequency [28].

The shapes of magnetic spectra also show obvious changes. The second magnetic spectrum shows a sharper shape than the other two spectra. The shapes of magnetic spectrums were proved strongly damped by the damping factor [34]. By fitting the magnetic spectra with theoretical spectra, the values of damping factor were found as 0.036, 0.025 and 0.044 for x = 0.057, 0.085 and 0.116. These results are in good agreement with the shape changes of the magnetic spectrum. It can be seen that the real part of permeability is more than 100 and 150 below 2.0 GHz, and the imaginary part gradually increases to a maximum at f = 3.61 GHz and 2.84 GHz for samples with x = 0.085 and 0.116, respectively. The high permeability and resonance frequency implies that the granular films are promising for applications in the high frequency range.

At last, we study the saturation magnetizations M_s and resistivities ρ of samples as a function of fraction of $Ni_{0.5}Zn_{0.5}Fe_2O_4$ x as shown in Figure 12. It can be obtained that M_s shows a linear decrease as x enlarges. It can be easily understood that M_s is equal to the total moment divided by volume and then the total moment decreases while atom fraction x increases. As x is the atom fraction and the molecular weight of ferrite is four times larger than $Co_{0.65}Fe_{0.35}$, the volume fraction is larger than the atom fraction. Resistivity ρ increases as x enlarges, which is caused by the more and more insulator fractions. The relationship between resistivity and x can be fitted by the percolation formula [35]

$$\rho \propto \rho_0 (1 - x - p_c)^{-\alpha} \quad (3)$$

where, ρ_0 is the resistivity of CoFe, p_c is the percolation threshold, and α is the critical exponent. The fitting results are also shown in Figure 12.

3 Summary

In summary, the good performance of the resonance frequency and the GHz permeability can be realized in metallic, ferrite and granular thin films with an easy magnetic plane in the film plane. Compared with the same bulk magnetic materials, the significant improvement of both the resonance frequency and the GHz permeability of the thin film were obtained from the formation of the special bianisotropy [8]. Besides a high saturation magnetization of the thin film, the adjustable in-plane anisotropic field is the key issue. In order to obtain a low energy loss of the thin films, a certain number of magnetic insulators distributed in the thin films seem to be a good choice.

By doping a small amount of Zr and Nb, the static and dynamic magnetic properties of a Co thin film deposited by oblique sputtering can be significantly optimized. Such an optimization is obtained, most likely, from the fact that when the size of Co grains decreases to a value lower than their exchange length, the exchange coupling between those grains will significantly weaken the magnetocrystalline anisotropy of the individual grain. Therefore, the 'obliquely induced' in-plane anisotropy, which can be easily manipulated by controlling the oblique deposition angle, can play a dominant role in determining the static and dynamic magnetic properties of the films. Thus, the intensity of the in-plane uniaxial anisotropic field as well as the high frequency performance of these films can be *in situ* designed.

Thus, we have succeeded in preparing single-phase NiZn ferrite films with different Ni contents having excellent soft magnetic properties with a spinel crystal structure using magnetron sputtering at room temperature, and showed that the microstructure, especial the grain size, the crystalline structure and growing pattern, plays a very important role in determining the magnetic characteristics of nanocrystalline NiZn ferrite films. All the films have exhibited relatively large μ' of 7–20.5 and high f_r of 1.85–4.3 GHz. Especially, the film with x = 0.70 achieved the f_r of 4.3 GHz, which is much higher than in the reports about soft ferrite films. The film with optimized x = 0.45 has high μ' of 15 and f_r of 2.8 GHz because of it having a large $\mu_0 M_s$ of 0.459 T. We could adjust the resonance frequency f_r of the ferrite films by changing the composition to satisfy the practical application.

Finally, $(Co_{0.65}Fe_{0.35})_{1-x}(Ni_{0.5}Zn_{0.5}Fe_2O_4)_x$ granular films have also been successfully fabricated by magnetron sputtering, and good soft magnetic properties have been obtained with high resistivity and high saturation magnetization. For the typical samples of x = 0.085 and x = 0.116, the resistivity reaches 677 μΩ cm and 1371 μΩ cm and saturation magnetization are 1.41 T and 1.19 T. At a frequency lower than 1.0 GHz, the real part of the complex relative permeability of these two samples are more than 100 and 150 and the resonance frequency reaches 3.61 GHz and 2.84 GHz, which implies that the films are promising for high frequency applications. These composite granular films show high resonance frequency, permeability and resistivity.

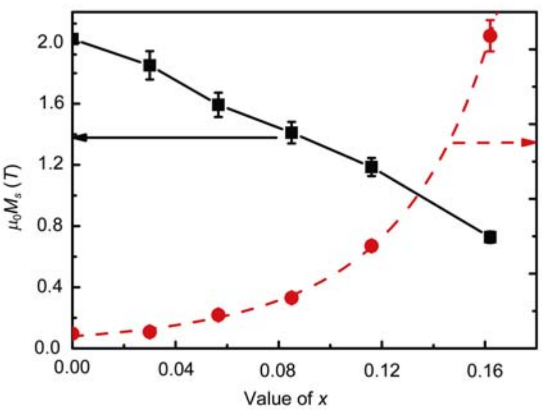

Figure 12 (Color online) Saturation magnetization $\mu_0 M_s$ and resistivity ρ as a function of the components of ferrites for $(Co_{0.65}Fe_{0.35})_{1-x}(Ni_{0.5}Zn_{0.5}Fe_2O_4)_x$ composite granular films [28].

This work was supported by the National Natural Science Foundation of China (Grant No. 11034004), National Science Fund for Distinguished Young Scholars (Grant No. 50925103), Key Grant Project of Chinese Ministry of Education (Grant No. 309027) and the Fundamental Research Funds for the Central Universities (Grant No. lzujbky-2010-219).

1 Wang S X, Sun N X, Yamaguchi M, et al. Sandwich films: Properties of a new soft magnetic material. Nature, 2000, 407: 150–151
2 Zhao Y W, Zhang X K, Xiao J Q. Submicrometer laminated Fe/SiO2 soft magnetic composites-an effective route to materials for high-frequency applications. Adv Mater, 2005, 17: 915–918
3 Yu S H, Yoshimura M. Ferrite/metal composites fabricated by soft solution processing. Adv Funct Mater, 2002, 12: 9–15
4 Naito Y, Suetaki K. Application of ferrite to electromagnetic wave absorber and its characteristics. IEEE Trans Microwave Theor Tech, 1971, 19: 65–72
5 Tang N J, Lu L Y, Zhong W. Synthesis and magnetic properties of carbon-coated Ni/SiO2 core/shell nanocomposites. Sci China Ser G-Phys Mech Astron, 2009, 52: 31–34
6 Chai G Z, Xue D S, Fan X L, et al. Extending the Snoek's limit of single layer film in $(Co_{96}Zr_4/Cu)_n$ multilayers. Appl Phys Lett, 2008, 93: 152516-1-3
7 Acher O, Adenot A L. Bounds on the dynamic properties of magnetic materials. Phys Rev B, 2000, 62: 11324–11327
8 Xue D S, Li F S, Fan X L, et al. Bianisotropy picture of higher permeability at higher frequencies. Chin Phys Lett, 2008, 25: 4120–4123
9 Kittel C. On the Theory of Ferromagnetic Resonance Absorption. Phys Rev, 1948, 73: 155–161
10 Zhang Z M, Fan X L, Lin M, et al. Optimized soft magnetic properties and high frequency characteristics of obliquely deposited Co–Zr thin films. J Phys D-Appl Phys, 2010, 43: 085002-1-4
11 Fan X L, Xue D S, Lin M, et al. In situ fabrication of CoNb soft magnetic thin films with adjustable resonance frequency from 1.3 to 4.9 GHz. Appl Phys Lett, 2008, 92: 222505-1-3
12 Zuo X, Yang A, Yoon S D, et al. Large induced magnetic anisotropy in manganese spinel ferrite films. Appl Phys Lett, 2005, 87: 152505-1-3
13 Wakiya N, Shinozaki K, Mizutani N. Stress-induced magnetization for epitaxial spinel ferrite films through interface engineering. Appl Phys Lett, 2004, 85: 1199–1201
14 Bohra M, Prasad S, Kumar N, et al. Large room temperature magnetization in nanocrystalline zinc ferrite thin films. Appl Phys Lett, 2006, 88: 262506-1-3
15 Koblischka M R, Kirsch M, Brust M, et al. Preparation of thin ferrite films on silicon using RF sputtering. Phys Status Solid, 2008, 205: 1783–1786
16 Desai M, Prasad S, Venkataramani N, et al. Anomalous variation of coercivity with annealing in nanocrystalline NiZn ferrite films. J Appl Phys, 2002, 91: 7592–7594
17 Bae S Y, Kim C S, Oh Y J. Magnetic properties of sol-gel derived Ni–Zn ferrite thin films on yttria stabilized zirconia buffered Si(100). J Appl Phys, 1999, 85: 5226–5228
18 Guo D W, Fan X L, Chai G Z, et al. Structural and magnetic properties of NiZn ferrite films with high saturation magnetization deposited by magnetron sputtering. Appl Surf Sci, 2010, 256: 2319–2322
19 Guo D W, Zhang Z M, Lin M, et al. Ni–Zn ferrite films with high resonance frequency in the gigahertz range deposited by magnetron sputtering at room temperature. J Phys D-Appl Phys, 2009, 42: 125006-1-4
20 Morikawa T, Suzuki M, Taga Y, et al. Soft magnetic properties of Co–Cr–O granular films. J Appl Phys, 1998, 83: 6664–6666
21 Ohnuma M, Hono K, Onodera H, et al. Microstructures and magnetic properties of Co–Al–O granular thin films. J Appl Phys, 2000, 87: 817–813
22 Ohnuma S, Lee H J, Kobayashi N, et al. Co-Zr-O nano-granular thin films with improved high frequency soft magnetic properties. IEEE Trans Magn, 2001, 37: 2251–2254
23 Hayakawa Y, Makino A, Fujimori H, et al. High resistive nanocrystalline Fe-M-O (M=Hf, Zr, rare-earth metals) soft magnetic films for high-frequency applications (invited). J Appl Phys, 1997, 81: 3747–3752
24 Ohnuma S, Fujimori H, Mitani S, et al. High-frequency magnetic properties in metal-nonmetal granular films (invited). J Appl Phys, 1996, 79: 5130–5135
25 Yao D S, Ge S H, Zhang B M, et al. Fabrication and magnetism of $Fe_{65}Co_{35}$-MgF_2 granular films for high frequency application. J Appl Phys, 2008, 103: 113901-1-3
26 Herzer G. Grain size dependence of coercivity and permeability in nanocrystalline ferromagnets. IEEE Trans Magn, 1990, 26: 1397–1402
27 Xue D S, Chai G Z, Li X L, et al. Effects of grain size distribution on coercivity and permeability of ferromagnets. J Magn Magn Mater, 2008, 320: 1541–1543
28 Chai G Z, Guo D W, Li X L, et al. Magnetic properties of $(Co_{0.65}Fe_{0.35})_{1-x}(Ni_{0.5}Zn_{0.5}Fe_2O_4)_x$ bi-magnetic composite granular films for high frequency application. J Phys D-Appl Phys, 2009, 42: 205006-1-6
29 Li W D, Kitakami O, Shimada Y. Study on the in-plane uniaxial anisotropy of high permeability granular films. J Appl Phys, 1998, 83: 6661–6663
30 Bekker V, Seemann K, Leiste H. A new strip line broad-band measurement evaluation for determining the complex permeability of thin ferromagnetic films. J Magn Magn Mater, 2004, 270: 327–332
31 Qian Z, Wang G, Sivertsen J M, et al. NiZn ferrite thin films prepared by Facing Target Sputtering. IEEE Trans Magn, 1997, 33: 3748–3750
32 Patterson A L. The Scherrer Formula for X-Ray Particle Size Determination. Phys Rev, 1939, 56: 978–982
33 Gilbert T L. A phenomenological theory of damping in ferromagnetic materials. IEEE Trans Magn, 2004, 40: 3443–3449
34 Liu Y, Tan C Y, Liu Z W, et al. Microstructure and high frequency properties of nanogranular CoAlO thin films. J Appl Phys, 2007, 101: 023912-1-5
35 Rosenbaum T F, Andres K, Thomas G A, et al. Sharp metal-insulator transition in a random solid. Phys Rev Lett, 1980, 45: 1723–1726